ERJ Express. Published on May 28, 2008 as doi: 10.1183/09031936.00064508

HO-1 plays a central role in NNK-mediated lung carcinogenesis

Running title: HO-1 in lung carcinogenesis

Ming-Yue Li[1], Johnson Yip[1], Michael KY Hsin[1], Tony SK Mok[2], Yilong Wu[3], Malcolm J Underwood[1], George G Chen[1]

[1]Department of Surgery, [2]Department of clinical Oncology, The Chinese University of Hong Kong, Prince of Wales Hospital, Shatin, N.T., Hong Kong.

[3]Lung Cancer Research Institute & Cancer Center, Guangdong Provincial People's Hospital, Guangdong, Guangzhou, China.

Correspondence to: George G Chen, Department of Surgery, The Chinese University of Hong Kong, Prince of Wales Hospital, Shatin, New Territories, Hong Kong. Tel: 852 2632 3934, Fax: 852 2645 0605, email:gchen@cuhk.edu.hk

Abstract

NNK, the tobacco-specific nitrosamine, is a potent lung cancer inducer. However, how NNK induces lung cancer is still largely unknown.

We evaluated HO-1 in 30 lung cancer tumor samples and their matched non-tumor tissues from patients with cigarette-smoking history. We also studied HO-1, p21, Bcl-2 families, MAPK and NF-κB expressions in lung cancer cells treated with NNK.

The level of HO-1 and p21 was significantly increased in lung tumor tissues. There was a positive relationship between these two proteins in the tumor. NNK stimulated the lung cell proliferation and elevated the levels of HO-1, p21, c-IAP2 and Bcl-2 but down-regulated Bad. These effects of NNK were blocked by ZnPP-XII, an HO-1 inhibitor. The NNK-mediated expression of HO-1 was governed by NF-κB and ERK1/2 since block of either prevented the stimulatory effect of NNK on HO-1 as well as HO-1 downstream molecules such as p21, c-IAP2, Bcl-2 and Bad.

In conclusion, HO-1 plays a central role in NNK-mediated cell proliferation by promoting the expression of p21, c-IAP2 and Bcl-2 but inhibiting the activity of Bad. NF-κB and ERK1/2 function at the up-stream of HO-1. Therefore, HO-1 is likely to be a potential target in the treatment of smoking-related lung cancer.

Key Words: ERK; HO-1; lung cancer; NF-κB; NNK

Introduction

Smoking is the single most extensively documented risk factor for all histological types of lung cancer [1]. Among the numerous toxic and carcinogenic agents in tobacco products, nicotine-derived 4-(*N*-methyl-*N*-nitrosoamino)-1-(3-pyridyl)-1-butanone (NNK) is the most potent carcinogen [2,3]. The total dose of NNK that is experienced by a smoker in a lifetime of smoking is remarkably close to the lowest dose that is shown to induce lung cancer in rats [3]. Clearly, NNK is a major contributor to lung carcinogenesis in smokers and secondhand smokers [4,5].

$p21^{Cip1/Waf1/Cid1}$ (p21) is best known for its ability to directly block the kinase activities of a broad range of cyclin/cyclin-dependent kinase (CDK) complexes in response to antimitogenic signals or DNA damage [6]. p21 can positively or negatively regulates the cell cycle and its role in carcinogenesis is inconsistent. The level of p21 is increased in various human cancers such as glioma cells, breast cancer, bladder cancer and pancreatic cancer [7,8]. The heme oxygenase (HO) system controls the rate-limiting step in heme catabolism. Three isoforms have been described. HO-2 and HO-3 are primarily constitutive, whereas HO-1 is highly inducible [9]. HO-1 has been shown to be associated with cell proliferation and growth and it participates in the pathogenesis of several types of cancers. An elevated expression or increased activity of HO-1 is associated with cellular proliferation in some tumors, such as prostate cancer, renal adenocarcinoma, gastric cancer and papillary thyroid cancer [10-13]. There is currently no work that describes the relationship between p21 and HO-1 in the lung cancer.

Nuclear factor-κB (NF-κB) is a collective designation for a family of highly regulated dimeric transcription factors. In resting cells, NF-κB, prototypically a heterodimer of p50 and p65

subunits, resides in the cytoplasm in an inactive form that is bound to the inhibitory protein IκB. Upon cellular activation, IκB is phosphorylated by an IκB kinase complex and proteolytically degraded by proteasomes, leading to the activation of NF-κB [14]. NF-κB then translocates into the nucleus, where it binds to the κB-binding motifs in the promoters or enhancers of the genes. NF-κB can regulate cell proliferation, apoptosis, and cell migration and it is constitutively activated in several types of cancer cells [15,16]. The mitogen-activated protein kinase (MAPK) family of proteins, including c-Jun NH_2-terminal kinase (JNK), extracellular signal-regulated kinase (ERK) and p38 MAP kinase, play an important role in cell survival and apoptosis. The activation of the MAPK pathway can be either antiapoptotic or proapoptotic, depending on the cellular context [17-19]. Considering the tumor-promoting effect of NNK in lung, it would be interesting to look into the roles of NF-κB and MAPK in NNK-mediated lung carcinogenesis.

In the present study, we found that HO-1 was constitutively expressed in human lung tumor tissues and it plays a central role in NNK-mediated cell proliferation. ERK and NF-κB may function at the upstream of HO-1 whereas p21 at the downstream of HO-1. The pro-proliferative HO-1 induced by NNK may finalize its effect via increasing Bcl-2 but decreasing Bad. The block of HO-1 significantly prevents the effect of NNK on lung cells.

Materials and Methods

Reagents. NNK was purchased from Chemsyn Science Laboratories (Lenexa, KS). NF-κB SN50 was obtained from CN Biosciences (La Jolla, CA). Protease Inhibitor Cocktail and FITC-conjugated immunoglobulins were supplied by Sigma Chemical (Saint Louis, MO). The antibodies against NF-κB p65, phosphor-IκB, IκB, HO-1, c-IAP2, p38, actin, and

horseradish peroxidase (HRP) conjugated secondary antibodies were provided by Santa Cruz Biotechnology (Santa Cruz, CA). The antibodies against Bad, phosphor-Bad (Ser136), phosphor-Bad (Ser112), phosphor-Bad (Ser155), phosphor-ERK1/2, phosphor-SAPK/JNK, phosphor-p38, and ERK1/2 were from Cell Signaling Technology (Beverly, MA.). The antibodies against Bcl-2, p21, and SAPK/JNK were supplied from ZYMED® Laboratories (South San Francisco, CA). PI and the ProLong Antifade solution were from Molecular Probes (Eugene, OR). The Colorimetric Enzyme Immunoassay for NF-κB kit was purchased from Oxford Biomedical Research (Oxford, MI). Pierce SuperBlock was obtained from Pierce Biotechnology (Rockford, IL). VECTOR ImmPRESS Universal Antibody Kit and Biotinylated Secondary Antibodies were provided by Vector Laboratories (Burlingame, CA).

Human lung tissue and Immunohistochemistry. Thirty pairs of human lung tumor and non-tumor tissues were obtained from lung cancer patients who underwent surgical resection in Prince of Wales Hospital, Hong Kong. Tumor tissue samples were taken from the central part of the tumors. Of the 30 patients, seventeen were current cigarette smokers with an average smoking history of 35 years and the other thirteen patients were previous cigarette smokers with an average smoking history of 28 years. All tumor and non-tumor tissue specimens were confirmed by histological examination. The tissue samples were stored in a liquid nitrogen tank until the experiments were performed. The samples included 10 pairs of squamous cell carcinoma tissues, 10 pairs of adenocarcinoma tissues, 5 pairs of large cell carcinoma tissues, and 5 pairs of poorly differentiated carcinoma tissues. The tissues were sectioned and the immunohistochemical staining was performed as described previously [20]. Briefly, after the section was blocked with SBT (Pierce SuperBlock supplemented with 0.05% Tween-20), it was incubated with primary antibodies (p21, HO-1) overnight. For the p21 antibody, tissue sections were treated by ImmPRESS reagent. For the HO-1 antibody,

the biotinylated second antibody in SBT was used. The sections were examined using the Zeiss Spot imaging system (Carl Zeiss, Jena, Germany).

Cell culture. The human non-small cell lung cancer cells, NCI-H23, were grown in 100 mm tissue culture disks as described previously [19].

Assessment of cell proliferation and cell death. Cell proliferation was measured by MTT as described previously [19]. Cell proliferation was further confirmed by the bromodeoxyuridine (BrdU) labeling DNA method and performed according to the manufacturer's instructions (Roche Applied Science, Penzberg, Germany). Apoptosis was determined by Flow Diagram of APO-DIRECT^{TM} Apoptosis assay kit (Chemicon international, San Diego, CA) as previously described [19].

Fluorescence-immunohistochemical staining and microscopy. Fluorescence-immunohistochemical staining was performed as described previously[21]. For p21, the nucleus was counter-stained with 600 nM DAPI. For NFκB, the nucleus was counter-stained cells with 0.5 μg/ml PI. The stained cells were examined using the Zeiss Spot imaging system (Carl Zeiss, Jena, Germany).

NF-κB transcriptional activity assay An NF-κB ELISA kit (Oxford, MI) was used. According to the manufacturer's protocol, we diluted the nuclear protein samples at 0.2 μg/μl in dilution buffer and incubated them in 96-well plates that were pre-coated with an immobilized oligonucleotide that contains a consensus-binding site for the NF-κB (p50 and p105 specific). NF-κB binding to the target oligonucleotide was detected by incubation with the primary antibody specific for the activated form of NF-κB (p50 and p105 specific),

followed by the anti-IgG horseradish peroxidase-conjugate and developing solution. The plate was placed in a colorimetric plate reader and read at 450 nm after the color developed and the reaction was ended.

Western blotting. The cytosolic and the nuclear protein fractions, and total protein were isolated and Western blot analysis were performed according to our previous publication [21]. A quantification of protein was carried out by densitometry analysis and the result was presented by the relative intensity based on actin normalization for total and cytosolic protein and on lamin B normalization for nuclear protein.

Statistical analysis. Statistical analysis was performed using SPSS version 14 (Chicago, IL). The Wilcoxon signed-ranks test was used to compare the differences of p21 and HO-1 expression between tumor and non-tumor lung tissues. The chi-square test was used to study the correlation of p21 and HO-1 expression in tumor tissues. In the cell line study, the data were presented as the means ± SD for at least three separate determinations for each group. The differences between the groups were examined for statistical significance using a one-way ANOVA followed by Student's *t* test. $P < 0.05$ was used to indicate a statistically significant difference.

Results

HO-1 and p21 expression in lung tumor and non-tumor tissues. We evaluated the HO-1 and p21 expression in 30 pairs of lung tumor and non-tumor tissues. The scores of the immunohistochemical staining (Table 1) showed that HO-1 and p21 levels were significantly increased in the tumor tissues compared with the non-tumor tissues (both $P < 0.001$). There

was a positive relationship between HO-1 and p21 in tumor tissues (P <0.01). The expression of HO-1 and p21 was obviously increased in tumor tissues, compared with non-tumor tissues (Fig.1). HO-1 was found in both the nuclear and the cytoplasm but p21 was mainly detected in the nucleus of the tumor tissues (Fig. 1A).

NNK-induced human lung cancer cell proliferation. To investigate the effects of NNK on the proliferation of human lung cancer cells, we analyzed cell proliferation by MTT assay. NNK significantly increased the cell viability of the NCI-H23 cells in a time-dependent manner (Fig. 2A). It appeared that the effect of NNK plateaued after its concentration reached a level that was higher than 10 μM. Consistent with the MTT assay results, DNA synthesis assay also showed the promoting effect of 10 μM NNK on cell proliferation in a time-dependent manner (Fig. 2B). It was reported that 7 μM concentration of NNK was corresponding approximately to the amount found in one pack of cigarettes [22]. NNK can reduce the pulmonary cytotoxicity against attack or damage[23], which might facilitate the chronic deposit of a higher amount of NNK or its metabolites locally. Considering these facts and our dose-responsive curve of NNK, we used 10 μM NNK in all the following experiments.

Upregulation of HO-1, p21, and c-IAP2 by NNK and the effect of NNK on Bcl-2 and Bad expression in NCI-H23 cells. Our result revealed that the levels of HO-1, p21, and c-IAP2 proteins were upregulated in a time-dependent manner by NNK (Fig. 3A). The increased level of HO-1 could be detected as early as 1 h after NNK treatment. A clear increase in p21 was not observed until 2 h after the treatment. The upregulated c-IAP2 protein expression appeared to occur much later than the above two molecules studied (Fig. 3A). Hence, the increased expression of HO-1 and p21 proteins occurred at earlier time points. Western blot

results clearly showed that NNK upregulated p21 expression in the nucleus (Fig. 3B). The accumulation of p21 in nucleus by NNK was further supported by the result of p21 fluorescence immunostaining (Fig. 4B), which is consistent with the results of the immunohistochemical staining of p21 in the tumor tissue (Fig. 1A).

Mammalian Bcl-2 and its closest relatives, such as Bcl-X_L and Bcl-w, Mcl-l, and A1, promote cell survival. In contrast, other members of the family such as Bax, Bid, Bak and Bad induce cell death [24]. Biologically active Bad is in a dephosphorylated form and it interacts with Bcl-2 and Bcl-XL to suppress their antiapoptotic function. By contrast, the inactive form of Bad is highly phosphorylated. It binds to 14-3-3 scaffold proteins and thus cannot interact with Bcl-2 or Bcl-XL [25]. Our results showed that NNK downregulated Bad expression and upregulated Bcl-2 expression in NCI-H23 cells in a time-dependent manner. The decreased Bad expression was obvious at 2 h after NNK treatment but the increased Bcl-2 was not observed until 4 or 8 h after the treatment (Fig. 3A), which indicates that the former occurred much earlier than the latter in lung cancer cells that were treated by NNK. NNK enhanced the levels of phospho-Bad (Ser112, Ser136, and Ser155) (Fig. 3B), which indicates that Bad was inactivated by NNK.

HO-1 functions as an upstream molecule to regulate p21 and apoptosis. The increased expression of HO-1 occurred at the earliest time point among HO-1, p21, and c-IAP2 (Fig. 3A), which suggests that the HO-1 signal was upstream of other molecular events. To confirm this, we applied ZnPP XII, a specific inhibitor of HO-1, to block HO-1 expression. Our results showed that ZnPP XII significantly inhibited not only HO-1 expression but also p21 and c-IAP2 expression in the cells treated with NNK (Fig. 4A), indicating that HO-1 is necessary for the maximal expression of p21 and c-IAP2 in NNK-treated cells. Furthermore,

our p21 fluorescence immunostaining demonstrated that the effect of NNK on p21 relocalization and accumulation in the nucleus could be blocked by ZnPP XII (Fig. 4B), which provides another piece of evidence that HO-1 may function to regulate p21. The inhibition of HO-1 level by ZnPP XII significantly blocked NNK-induced cell proliferation (Fig. 4C). In addition, such an inhibition also significantly promoted cellular apoptosis even in the presence of NNK (Fig. 4D). These data clearly supported that HO-1 as well as its downstream p21 played the positive role in NNK-induced cell proliferation.

Activation of NF-κB and MAPK in NNK-treated NCI-H23 cancer cells. NF-κB is constitutively activated in several types of cancer cells [15,16]. In addition, reports have shown that NNK activates the NF-κB in macrophages [26] and that NF-κB is involved in the growth of colon cancer and oral cancer cells [27,28]. However, few studies have addressed the relationship between NNK and NF-κB in lung cancer. Therefore, we examined whether NF-κB activation could be induced by NNK in NCI-H23 lung cancer cells. The experiments showed that lung cancer cells constitutively expressed the p65 subunit of NF-κB (Fig. 5A-C). NNK not only upregulated the expression of p65 protein but also increased its translocation into the nucleus, which was detectable as early as 30 min after the treatment and peaked 2 h after the treatment (Fig. 5A). The translocation of p65 into the nucleus was confirmed by immunofluorescence assay (Fig. 5B). The profiles of elevated p65 protein and its nuclear translocation were further supported by the time-course study of NF-κB transcriptional activity, in which its activity peaked 2 h after the treatment (Fig. 5C). Consistent with above data, the phosphorylated IκB (pIκB) also increased in the cytosol (Fig. 5A). The increase of pIκB in the cytosol may promote the translocation of NF-κB into the nucleus [14].

Western Blotting result showed that NNK significantly increased pERK1/2 protein as early as 30 min after NNK treatment, and its level peaked 60 min after treatment (Fig. 5D), which suggests that the increase in ERK1/2 activation is an early event in the NNK-mediated signal pathway in lung cancer cells. However, p38 and SAPK/JNK activation were not altered by NNK in the cells that were tested.

Regulation of HO-1, p21, c-IAP-2, Bad and Bcl-2 expression by the ERK kinase inhibitor and NF-κB inhibitor and ERK activation upstream of NF-κB activation in NNK-treated cells. As the results in Fig. 3 show, the levels of HO-1, p21, c-IAP2, and Bcl-2 proteins were enhanced by NNK. However, such a promoting effect was prevented by U0126, a specific inhibitor of ERK activation or SN50, a specific inhibitor of NF-κB activation (Fig. 6A). In contrast, the level of Bad was reduced by NNK (Fig. 3). This reduction effect was inhibited by either U0126 or SN50 (Fig. 6A). Hence, the data suggest that the regulation of these proteins by NNK may require the activation of ERK and NF-κB. To further assess the role of NF-κB and ERK in NNK-treated cells, U0126 and SN50 were employed to study the relationship between the activity of NF-κB and ERK activation. It was found that both U0126 and SN50 significantly blocked NNK-mediated NF-κB transcriptional activity, which resulted in the reduction of its activity to the control level (Fig. 6B). NNK-mediated ERK activation was prevented by U0126 but not by SN50 (Fig. 6C). The results suggest that ERK activation probably functions upstream of NF-κB in the NNK-mediated pathway. This suggestion is in line with our time-course studies of ERK and NF-κB, which showed that the maximal activity of NF-κB that was induced by NNK occurred 2 h after NNK treatment, whereas the peak level of pERK was observed 1 h earlier (Figs. 5).

Discussion

HO-1 participates in the development of some malignant tumors such as gastric cancer and thyroid carcinoma [12,13]. The inhibition of HO-1 reduces the growth of lung tumor in mice [29]. Our present study found that the HO-1 was significantly increased in the lung tumor tissue of smokers and that cigarette carcinogen NNK was able to stimulate the expression of HO-1 protein. The result suggests that an increase in HO-1 may be a key molecule in the development of the cigarette smoking-related lung cancer. And this conclusion is reinforced by the findings that the block of HO-1 prevents NNK-induced cell proliferation and reduces the growth of lung cancer. In this study, variety of HO-1 upstream and downstream molecules has been found to associate with NNK treatment and this supports the central role of HO-1 in NNK-mediated lung carcinogenesis.

NF-κB appears to be an upstream molecule in NNK-mediated HO-1 expression. As in many other types of cells [15,16], we found that there was a constitutive NF-κB activity in the NCI-H23 lung cancer cells. Despite the well-known prosurvival/growth effect of NF-κB, there is very limited information on the relation between NF-κB and the tobacco-specific carcinogenic agent NNK in human lung cancer. Our present study demonstrated that NNK increased the activity of NF-κB significantly, as evidenced by the increase of its subunit p65 protein, the nuclear translocation of p65, and the elevated transcriptional activity in non-small cell lung cancer cells (NSCLC) NCI-H23. The elevated activity of NF-κB was accompanied by an increased proliferation and growth of lung cancer cells treated by NNK. This elevation of NF-κB activity was observed as early as 15 minutes after NNK treatment and the maximal effect was recorded 2 hours after NNK treatment, which indicates that the increase in NF-κB activity was a relatively early event in the NNK-mediated signal transduction pathway. The nuclear NF-κB transactivates a large body of genes that are involved in diverse cellular

functions, such as cell proliferation, apoptosis inhibition, cell adhesion, and cell migration [30]. These diverse cellular functions can be regulated by MAPK, the activity of which is closely associated with NF-κB [12,13]. In the present study, we demonstrated that NNK significantly stimulated the ERK activation in lung cancer cells. Furthermore, the time-course study demonstrated that the change in ERK predated the increased NF-κB activity. This observation was further supported by the experiment that employed an ERK inhibitor (U0126) and an NF-κB inhibitor (SN50). Both U0126 and SN50 effectively blocked most of the NF-κB transcriptional activity that was induced by NNK. However, NNK-mediated increased ERK activation was prevented only by U0126 and not by SN50. Therefore, ERK appears to function upstream of NF-κB in NNK-treated NCI-H23 cells. In fact, NNK has been documented to promote the activity of NF-κB in human bronchial epithelial cells [31], although it has not been shown which subunit of NF-κB contributes to the increased activity. Our study has indicated that NNK affects the multiple steps that are related to the activity of NF-κB. It increases the p65 subunit of NF-κB, promotes its nuclear translocation and stimulates its transcriptional activity. The increased p65 subunit observed in this study is supported by the fact that this p65 protein is overexpressed in lung tissue samples of NSCLC [32]. It is noted that a previous study failed to show that NNK can stimulate the activity of NF-κB in NSCLC cells [33]. The concentration of NNK that was used in this previous study was 100 nM, which is much lower than the 10 μM that was employed in the present study. The difference in the NNK concentration used is likely the factor that is responsible for the different results that were obtained between the previous study and our study. The concentration of 10 μM NNK used in the present study is in line with a report that shows that the same concentration of NNK also promotes the activity of NF-κB[31]. More importantly, NNK at a concentration of 10 μM is achievable in smokers[22,23]. Concentrations of

nicotine have been reported in the range of 10–100 μM in serum[34], and even higher on the local mucosal surface [35].

Our study demonstrated that the level of HO-1 was governed by ERK and NF-κB, as both U0126 and SN50, potent inhibitors of ERK and NF-κB respectively, prevented the expression of HO-1 that was induced by NNK. These results strongly indicate that NF-κB and ERK activation is necessary for NNK to stimulate the expression of HO-1 in the NSCLC cells tested. Our findings are supported by the observations that the MAPK pathway and NF-κB appear to be involved in HO-1 expression in response to diverse stimuli [12,36], and that the inhibition of the ERK/MAPK pathway attenuates HO-1 expression [37].

The first HO-1 downstream molecule in NNK-mediated pathway is p21. p21 is defined as a negative cell cycle regulator because it binds cyclin-dependent kinases and regulates the activity of these molecules in the early G_1 phase. In normal cells, its function is to ensure appropriate cyclin-dependent kinase inhibition during cell cycle progression. However, recent studies have demonstrated that p21 may also have an antiapoptotic function, which enables the cells to proliferate under conditions that otherwise lead to apoptosis or arrest[8,38]. There has been no report of the relationship between p21 and lung cancer patients with cigarette-smoking history. In the present study, we have demonstrated that the nuclear p21 significantly increased in the lung tumor tissues from the smokers, suggesting that p21 may play a role in lung cancer. The finding is in line with a recent publication showing a positive role of p21 in lung cancer cell proliferation [39]. Our study has further revealed that there is a positive relationship between the expression of p21 and HO-1 in lung cancer. The time-course study showed that the increase of HO-1 occurred earlier than the elevated expression of p21 in NNK-treated cells. ZnPP XII, a HO-1-specific inhibitor, not

only decreased HO-1 expression but also downregulated p21 expression in NNK-treated cells, which suggests that HO-1 functions upstream of p21. Previous studies of solid tumors have indicated that the overexpression of HO-1 results in a significant increase in the level of p21 and that subsequently it renders tumor cells resistant to cell death stimulation [12,13]. Similar to the case for HO-1, the increased level of p21 in the NNK-treated cells could also be inhibited by either ERK inhibitor U0126 or NF-κB inhibitor SN50. The tumor-promoting effect of p21 is MARK-dependent[8,40]. Collectively, our results demonstrate that p21 is a downstream molecule of HO-1 and both HO-1 and p21 are governed by ERK and NF-κB in the NNK-mediated HO-1 pathway.

Another molecule that is possible downstream of HO-1 in NNK-treated lung cancer cells is Bcl-2. NNK can stimulate the expression of Bcl-2 protein in NSCLC cells. Similar to the regulation of p21 by NNK, an increased level of Bcl-2 can be prevented by the ERK inhibitor U0126 and the NF-κB inhibitor SN50, which indicates that the increased level of Bcl-2 is controlled by ERK and NF-κB, both of which function upstream of HO-1. Therefore, ERK and NF-κB may influence the level of Bcl-2 via the promotion of HO-1 in NSCLC cells. The role of HO-1 in the regulation of Bcl-2 is supported by the finding that the level of Bcl-2 can be upregulated by the exogenous transfer of HO-1 into cells[41]. In addition to HO-1, the production of Bcl-2 may also be regulated by NF-κB because the promoter region of Bcl-2 contains binding sites for NF-κB. The stimulation of the binding site may induce the generation of Bcl-2[42].

NNK has been shown to downregulate the expression of Bad but to upregulate the level of c-IAP2 in NSCLC cells. The finding of decreased Bad and the increased c-IAP2 is in agreement with the cell-growth promotive feature of NNK, as the Bad can function to induce

cell death whereas the c-IAP2 can function to inhibit it. Biologically active Bad is in a dephosphorylated form and it interacts with Bcl-2 and Bcl-XL to suppress their antiapoptotic function. In contrast, the inactive form of Bad is highly phosphorylated. It binds to 14-3-3 scaffold proteins and cannot interact with Bcl-2 or Bcl-XL [25]. Interestingly, NNK has been known to strongly induce the phosphorylation of Bad at multiple sites, including Ser112, Ser136, and Ser155, and the phosphorylation of Bad is associated with the increased survival of human lung cancer cells [43]. Our study indicated that U0126 and SN50, the potent inhibitors of ERK and NF-κB respectively, prevented the effect of NNK on Bad and c-IAP2 expression. c-IAP2 appears to be a downstream molecule of HO-1 and p21, as the expression of HO-1 and p21 predates the increase of c-IAP2. Although the way in which HO-1 and p21 interact with c-IAP2 is not clear, the IAP molecule is known to participate in the antiapoptotic pathway of ERK [12,44].

In conclusion, our study shows increased level of HO-1 in lung tumor tissues of the smokers and NNK-treated cells, which suggests a positive role of this protein in smoking-mediated lung carcinogenesis. The NNK-mediated expression of HO-1 requires ERK and NF-κB since the inhibition of either prevents the effect of NNK on HO-1 expression. The elevated HO-1 by NNK may function to stimulate p21 expression, which subsequently inhibits Bcl-2, activates Bad, and leads to the proliferation of lung cancer cells. Such a series of reaction is blocked when HO-1 is inhibited. The central role of HO-1 in NNK-mediated lung carcinogenesis suggests that HO-1 be a potential target in lung cancer prevention and treatment.

Acknowledgements

We thank Mr. Ernest Chak for technical assistance in immunochemical staining. The study was in part supported by a direct grant (2041304) from the CUHK.

References

1. Stellman SD, Takezaki T, Wang L, Chen Y, Citron ML, Djordjevic MV, Harlap S, Muscat JE, Neugut AI, Wynder EL, Ogawa H, Tajima K, Aoki K. Smoking and lung cancer risk in American and Japanese men: an international case-control study. *Cancer Epidemiol Biomarkers Prev* 2001; 10: 1193-9.

2. Hecht SS, Hoffmann D. Tobacco-specific nitrosamines, an important group of carcinogens in tobacco and tobacco smoke. *Carcinogenesis* 1988; 9: 875-84.

3. Hoffmann D, Rivenson A, Hecht SS. The biological significance of tobacco-specific N-nitrosamines: smoking and adenocarcinoma of the lung. *Crit Rev Toxicol* 1996; 26: 199-211.

4. Schuller HM. Mechanisms of smoking-related lung and pancreatic adenocarcinoma development. *Nat Rev Cancer* 2002; 2: 455-63.

5. Schuller HM, Plummer HK 3rd, Jull BA. Receptor-mediated effects of nicotine and its nitrosated derivative NNK on pulmonary neuroendocrine cells. *Anat Rec A Discov Mol Cell Evol Biol* 2003; 270: 51-8.

6. Sherr CJ, Roberts JM. CDK inhibitors: positive and negative regulators of G1-phase progression. *Genes Dev* 1999; 13: 1501-12.

7. Hiyama H, Iavarone A, Reeves SA. Regulation of the cdk inhibitor p21 gene during cell cycle progression is under the control of the transcription factor E2F. *Oncogene* 1998; 16: 1513-23.

8. Rosetti M, Zoli W, Tesei A, Ulivi P, Fabbri F, Vannini I, Brigliadori G, Granato AM, Amadori D, Silvestrini R. Iressa strengthens the cytotoxic effect of docetaxel in NSCLC models that harbor specific molecular characteristics. *J Cell Physiol* 2007; 212: 710-6.

9. McCoubrey WK Jr, Huang TJ, Maines MD. Isolation and characterization of a cDNA from the rat brain that encodes hemoprotein heme oxygenase-3. *Eur J Biochem* 1997; 247: 725-32.

10. Maines MD, Abrahamsson PA. Expression of heme oxygenase-1 (HSP32) in human prostate: normal, hyperplastic, and tumor tissue distribution. *Urology* 1996; 47: 727-33.

11. Goodman AI, Choudhury M, da Silva JL, Schwartzman ML, Abraham NG. Overexpression of the heme oxygenase gene in renal cell carcinoma. *Proc Soc Exp Biol Med* 1997; 214: 54-61.

12. Liu ZM, Chen GG, Ng EK, Leung WK, Sung JJ, Chung SC. Upregulation of heme oxygenase-1 and p21 confers resistance to apoptosis in human gastric cancer cells. *Oncogene* 2004; 23: 503-13.

13. Chen GG, Liu ZM, Vlantis AC, Tse GM, Leung BC, van Hasselt CA. Heme oxygenase-1 protects against apoptosis induced by tumor necrosis factor-alpha and cycloheximide in papillary thyroid carcinoma cells. *J Cell Biochem* 2004; 92: 1246-56.

14. Chen Z, Hagler J, Palombella VJ, Melandri F, Scherer D, Ballard D, Maniatis T. Signal-induced site-specific phosphorylation targets I kappa B alpha to the ubiquitin-proteasome pathway. *Genes Dev* 1995; 9: 1586-97.

15. Cavin LG, Romieu-Mourez R, Panta GR, Sun J, Factor VM, Thorgeirsson SS, Sonenshein GE, Arsura M. Inhibition of CK2 activity by TGF-beta1 promotes IkappaB-alpha protein stabilization and apoptosis of immortalized hepatocytes. *Hepatology* 2003; 3**8**: 1540-51.

16. Hideshima T, Chauhan D, Hayashi T, Akiyama M, Mitsiades N, Mitsiades C, Podar K, Munshi NC, Richardson PG, Anderson KC. Proteasome inhibitor PS-341 abrogates IL-6 triggered signaling cascades via caspase-dependent downregulation of gp130 in multiple myeloma. *Oncogene* 2003; 22: 8386-93.

17. Keshamouni VG, Reddy RC, Arenberg DA, Joel B, Thannickal VJ, Kalemkerian, GP, Standiford TJ. Peroxisome proliferator-activated receptor-gamma activation inhibits tumor progression in non-small-cell lung cancer. *Oncogene* 2004; 23: 100-8.

18. Yu W, Liao QY, Hantash FM, Sanders BG, Kline K. Activation of extracellular signal-regulated kinase and c-Jun-NH(2)-terminal kinase but not p38 mitogen-activated protein kinases is required for RRR-alpha-tocopheryl succinate-induced apoptosis of human breast cancer cells. *Cancer Res* 2001; 61: 6569-76.

19. Li M, Lee TW, Mok TS, Warner TD, Yim AP, Chen GG. Activation of peroxisome proliferator-activated receptor-gamma by troglitazone (TGZ) inhibits human lung cell growth. *J Cell Biochem* 2005; 96: 760-74.

20. Chen GG, Lai PB, Chak EC, Xu H, Lee KM, Lau WY. Immunohistochemical analysis of pro-apoptotic Bid level in chronic hepatitis, hepatocellular carcinoma and liver metastases. *Cancer Lett* 2001; 172: 75-82.

21. Li M, Lee TW, Yim AP, Mok TS, Chen GG. Apoptosis induced by troglitazone is both peroxisome proliferator-activated receptor-gamma- and ERK-dependent in human non-small lung cancer cells. *J Cell Physiol* 2006; 209: 428-38.

22. Proulx LI, Gaudreault M, Turmel V, Augusto LA, Castonguay A, Bissonnette EY. 4-(Methylnitrosamino)-1-(3-pyridyl)-1-butanone, a component of tobacco smoke, modulates mediator release from human bronchial and alveolar epithelial cells. *Clin Exp Immunol* 2005; 140: 46-53.

23. Proulx LI, Pare G, Bissonnette EY. Alveolar macrophage cytotoxic activity is inhibited by 4-(methylnitrosamino)-1-(3-pyridyl)-1-butanone (NNK), a carcinogenic component of cigarette smoke. *Cancer Immunol Immunother* 2007; 56: 831-8.

24. Print CG, Loveland KL, Gibson L, Meehan T, Stylianou A, Wreford N, de Kretser D, Metcalf D, Kontgen F, Adams JM, Cory S. Apoptosis regulator bcl-w is essential for spermatogenesis but appears otherwise redundant. *Proc Natl Acad Sci U S A* 1998; 95: 12424-31.

25. Scheid MP, Schubert KM, Duronio V. Regulation of bad phosphorylation and association with Bcl-x(L) by the MAPK/Erk kinase. *J Biol Chem* 1999; 274: 31108-13.

26. Rioux N, Castonguay A. The induction of cyclooxygenase-1 by a tobacco carcinogen in U937 human macrophages is correlated to the activation of NF-kappaB. *Carcinogenesis* 2000; 21: 1745-51.

27. Ye YN, Liu ES, Shin VY, Wu WK, Cho CH. The modulating role of nuclear factor-kappaB in the action of alpha7-nicotinic acetylcholine receptor and cross-talk between 5-lipoxygenase and cyclooxygenase-2 in colon cancer growth induced by 4-(N-methyl-N-nitrosamino)-1-(3-pyridyl)-1-butanone. *J Pharmacol Exp Ther* 2004; 311: 123-30.

28. Sawhney M, Rohatgi N, Kaur J, Shishodia S, Sethi G, Gupta SD, Deo SV, Shukla NK, Aggarwal BB, Ralhan R. Expression of NF-kappaB parallels COX-2 expression in oral precancer and cancer: association with smokeless tobacco. *Int J Cancer* 2007; 120: 2545-56.

29. Hirai K, Sasahira T, Ohmori H, Fujii K, Kuniyasu H. Inhibition of heme oxygenase-1 by zinc protoporphyrin IX reduces tumor growth of LL/2 lung cancer in C57BL mice. *Int J Cancer* 2007; 120: 500-5.

30. Pahl HL. Activators and target genes of Rel/NF-kappaB transcription factors. *Oncogene* 1999; 18: 6853-66.

31. Ho YS, Chen CH, Wang YJ, Pestell RG, Albanese C, Chen RJ, Chang MC, Jeng JH, Lin SY, Liang YC, Tseng H, Lee WS, Lin JK, Chu JS, Chen LC, Lee CH, Tso WL, Lai YC, Wu CH. Tobacco-specific carcinogen 4-(methylnitrosamino)-1-(3-pyridyl)-1-butanone (NNK) induces cell proliferation in normal human bronchial epithelial cells through NFkappaB activation and cyclin D1 up-regulation. *Toxicol Appl Pharmacol* 2005; 205: 133-48.

32. Denlinger CE, Rundall BK, Jones DR. Modulation of antiapoptotic cell signaling pathways in non-small cell lung cancer: the role of NF-kappaB. *Semin Thorac Cardiovasc Surg* 2004; 16: 28-39.

33. Tsurutani J, Castillo SS, Brognard J, Granville CA, Zhang C, Gills JJ, Sayyah J, Dennis PA. Tobacco components stimulate Akt-dependent proliferation and NFkappaB-dependent survival in lung cancer cells. *Carcinogenesis* 2005; 26: 1182-95.

34. Russell MA, Jarvis M, Iyer R, Feyerabend C. Relation of nicotine yield of cigarettes to blood nicotine concentrations in smokers. *Br Med J* 1980; 280: 972-6.

35. Turner DM, Armitage AK, Briant RH, Dollery CT. Metabolism of nicotine by the isolated perfused dog lung. *Xenobiotica* 1975; 5: 539-51.

36. Gong P, Cederbaum AI, Nieto N. Increased expression of cytochrome P450 2E1 induces heme oxygenase-1 through ERK MAPK pathway. *J Biol Chem* 2003; 278: 29693-700.

37. Benvenisti-Zarom L, Chen-Roetling J, Regan RF Inhibition of the ERK/MAP kinase pathway attenuates heme oxygenase-1 expression and heme-mediated neuronal injury. *Neurosci Lett* 2006; 398: 230-4.

38. LaRue KE, Khalil M, Freyer JP. Microenvironmental regulation of proliferation in multicellular spheroids is mediated through differential expression of cyclin-dependent kinase inhibitors. *Cancer Res* 2004; 64: 1621-31.

39. Bae KM, Wang H, Jiang G, Chen MG, Lu L, Xiao L. Protein kinase C epsilon is overexpressed in primary human non-small cell lung cancers and functionally

required for proliferation of non-small cell lung cancer cells in a p21/Cip1-dependent manner. *Cancer Res* 2007; 67: 6053-63.

40. Dent P, Grant S. Pharmacologic interruption of the mitogen-activated extracellular-regulated kinase/mitogen-activated protein kinase signal transduction pathway: potential role in promoting cytotoxic drug action. *Clin Cancer Res* 2001; 7: 775-83.

41. Zhang X, Shan P, Qureshi S, Homer R, Medzhitov R, Noble PW, Lee PJ. Cutting edge: TLR4 deficiency confers susceptibility to lethal oxidant lung injury. *J Immunol* 2005; 175: 4834-8.

42. Pozo-Guisado E, Merino JM, Mulero-Navarro S, Lorenzo-Benayas MJ, Centeno F, Alvarez-Barrientos A, Fernandez-Salguero PM. Resveratrol-induced apoptosis in MCF-7 human breast cancer cells involves a caspase-independent mechanism with downregulation of Bcl-2 and NF-kappaB. *Int J Cancer* 2005; 115: 74-84.

43. Jin Z, Xin M, Deng X. Survival function of protein kinase C{iota} as a novel nitrosamine 4-(methylnitrosamino)-1-(3-pyridyl)-1-butanone-activated bad kinase. *J Biol Chem* 2005; 280: 16045-52.

44. Erhardt P, Schremser EJ, Cooper GM. B-Raf inhibits programmed cell death downstream of cytochrome c release from mitochondria by activating the MEK/Erk pathway. *Mol Cell Biol* 1999; 19: 5308-15.

Table. 1. p21 and HO-1 and p21 expression in lung tissues from patients with lung cancer

Patient	p21 staining score		HO-1 staining score		statistical analysis	
No.	tumor	non-tumor	tumor	non-tumor	factors and methods	P
1	3	1	1	0		
2	4	2	1	0	p21 expression versus	
3	1	0	0	0	types of lesion (tumor	< 0.001
4	4	1	1	0	and non-tumor)	
5	1	0	1	0	*(Wilcoxon signed ranks test)*	
6	0	0	0	0		
7	1	0	1	0		
8	1	0	0	0		
9	4	1	0	0		
10	3	0	2	0	HO-1 expression versus	
11	2	1	2	0	types of lesion(tumor	<0.001
12	2	0	2	0	and non-tumor)	
13	2	2	4	0	*(Wilcoxon signed ranks test)*	
14	1	0	1	0		
15	1	0	0	0		
16	3	1	0	0		
17	2	0	1	0	p21 expression versus	
18	2	0	1	0	HO-1expression in	<0.01
19	2	1	1	0	tumor	
20	2	0	1	0	*(Chi-Square Test)*	
21	4	2	1	0		
22	2	1	0	0		
23	5	1	0	0		
24	3	1	2	0		
25	2	3	2	0		
26	3	1	0	0		
27	2	4	1	0		
28	2	1	1	1		
29	2	0	2	0		
30	3	1	2	0		

No.1-10: squamous cell carcinoma; No.11-20: adenocarcinoma; No.21-25: large cell carcinoma; No.26-30: poorly differentiated carcinoma.

The overall immunohistochemical staining was assessed by the values that were observed for the distribution of positive staining as follows: 0, no staining; 1, <20% of cells; 2, 21-40% of cells; 3, 41-60% of cells; 4, 61-80% of cells; 5, >81% of cells.

Figure legend

Fig. 1. HO-1 and p21 expression in human lung tumor and non-tumor tissues. The stained tissues were examined using the Zeiss Spot imaging system. The representative immunohistochemical stainings showed a significant increase in HO-1 levels in both the nucleus and the cytoplasm (Fig 1A) in the tumor tissues of all four types of lung cancers, compared with the matched non-tumor tissues. The positive staining of p21 was mainly in the nucleus of the tumor tissues (Fig. 1B) (original magnification x400). Adenocarcinoma: **A, B, I, J**. Squamous cell carcinoma: **C, D, K, L.** Poorly differentiated carcinoma: **E, F, M, N**. Large cell carcinoma: **G, H, O, P.**

Figure 1A

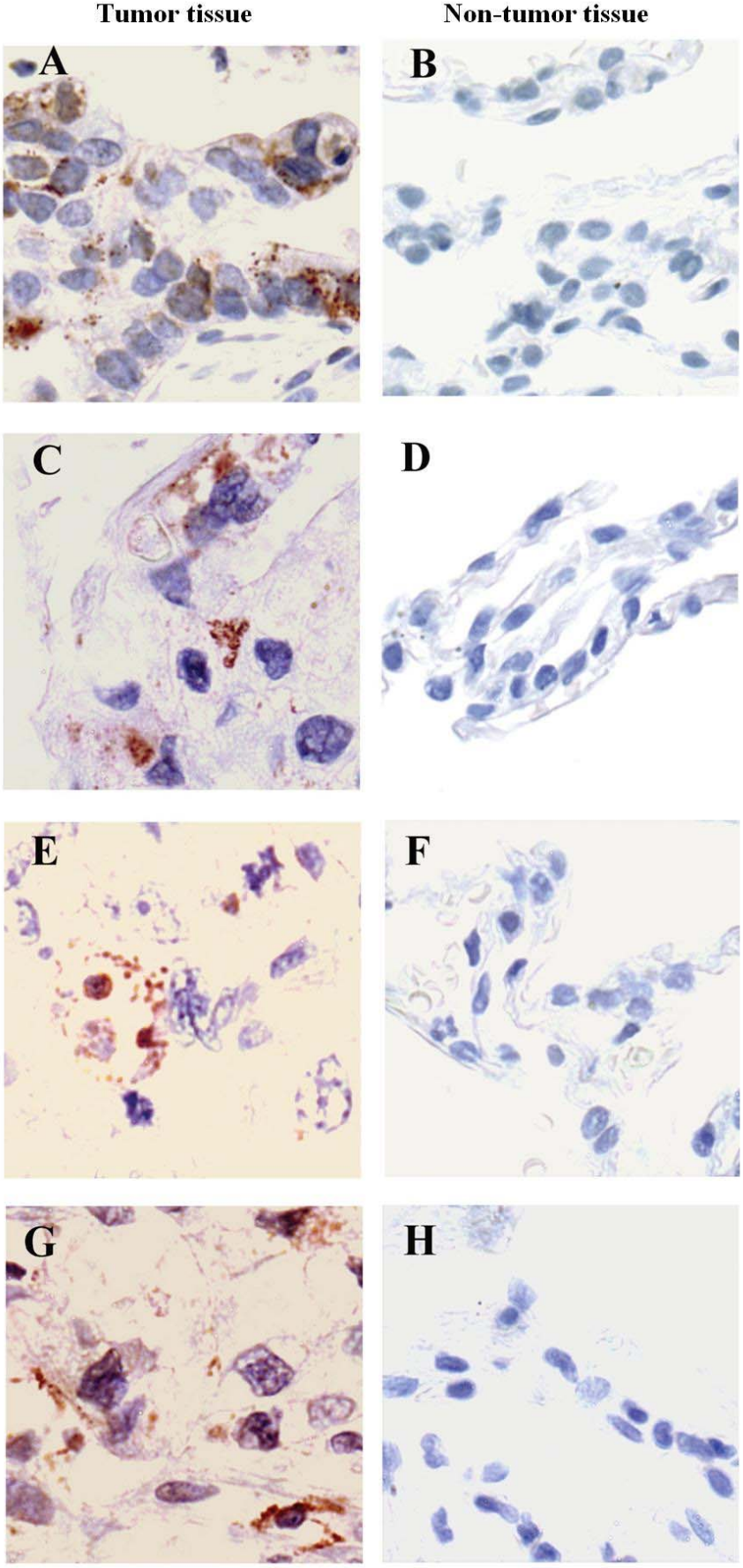

Figure 1B

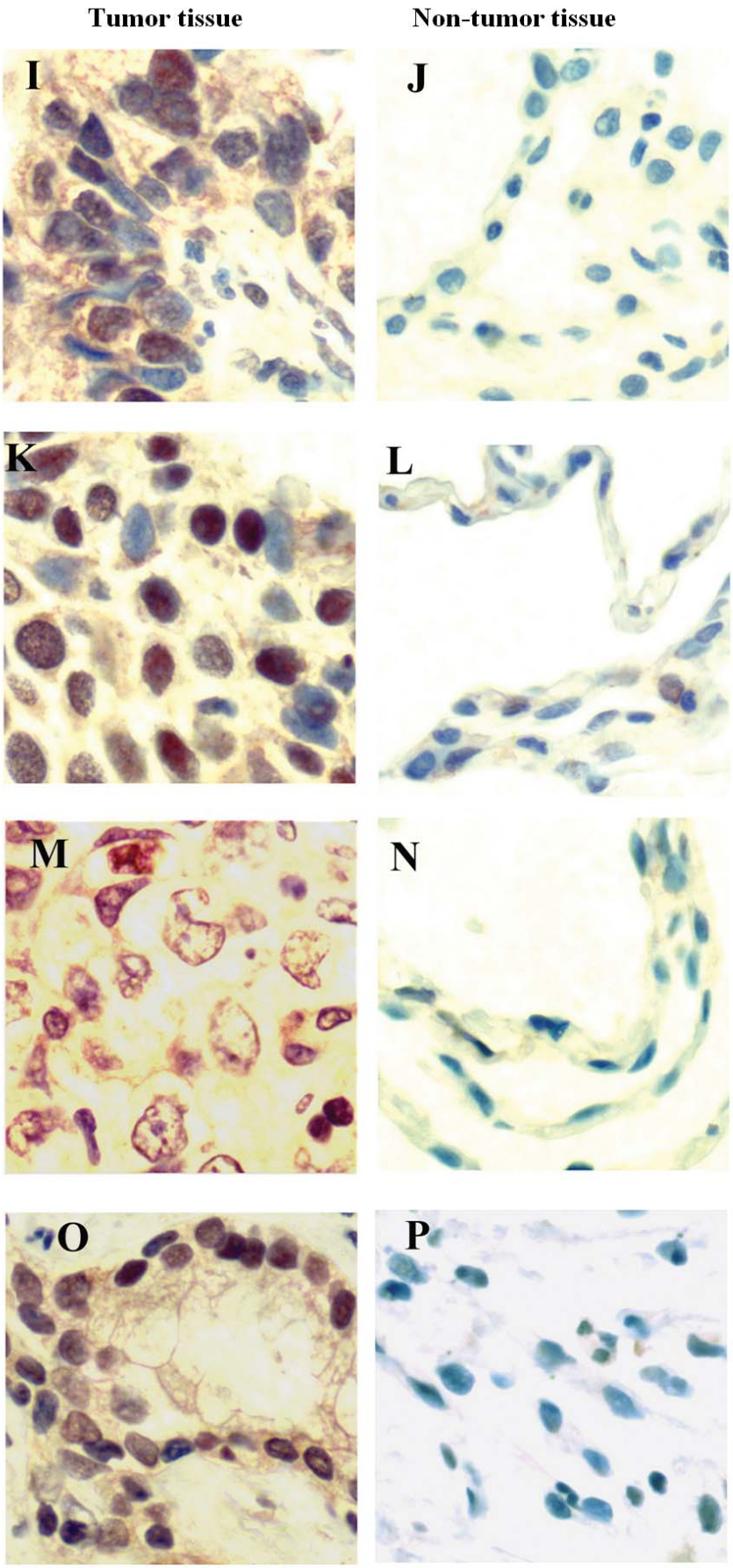

Fig. 2. NNK-induced the proliferation of lung cancer cells. **(A)** NCI-H23 cells were treated with NNK (0–500 μM) for 24 h, 48 h, and 72 h. Cell proliferation was measured by MTT assay and the data were expressed as a percentage of the control culture conditions (0 μM NNK). The data were represented as the mean ± SD for four replicate determinations for each treatment. The experiments were repeated twice with similar results. Compared with untreated cells, there was a significant increase in cells after 24 h ,48 h and 72 h of treatment with 10 μM NNK (□$p < 0.05$, ** $P < 0.01$, $n = 4$). **(B)** NCI-H23 cells were treated with NNK 10 μM for 0 h, 12 h, 24 h, 48 h, and 72 h. Cell proliferation determined by BrdU cell proliferation assay. The result was presented as the percentage of the 0 h control conditions. The data were represented as the mean ± SD for four replicate determinations for each treatment. The experiments were repeated twice with similar results. Compared with untreated cells, there was a significant increase in cells after 24 h, 48 h and 72 h of treatment with 10 μM NNK (□$p < 0.05$, ** $P < 0.01$, $n = 4$).

Figure 2

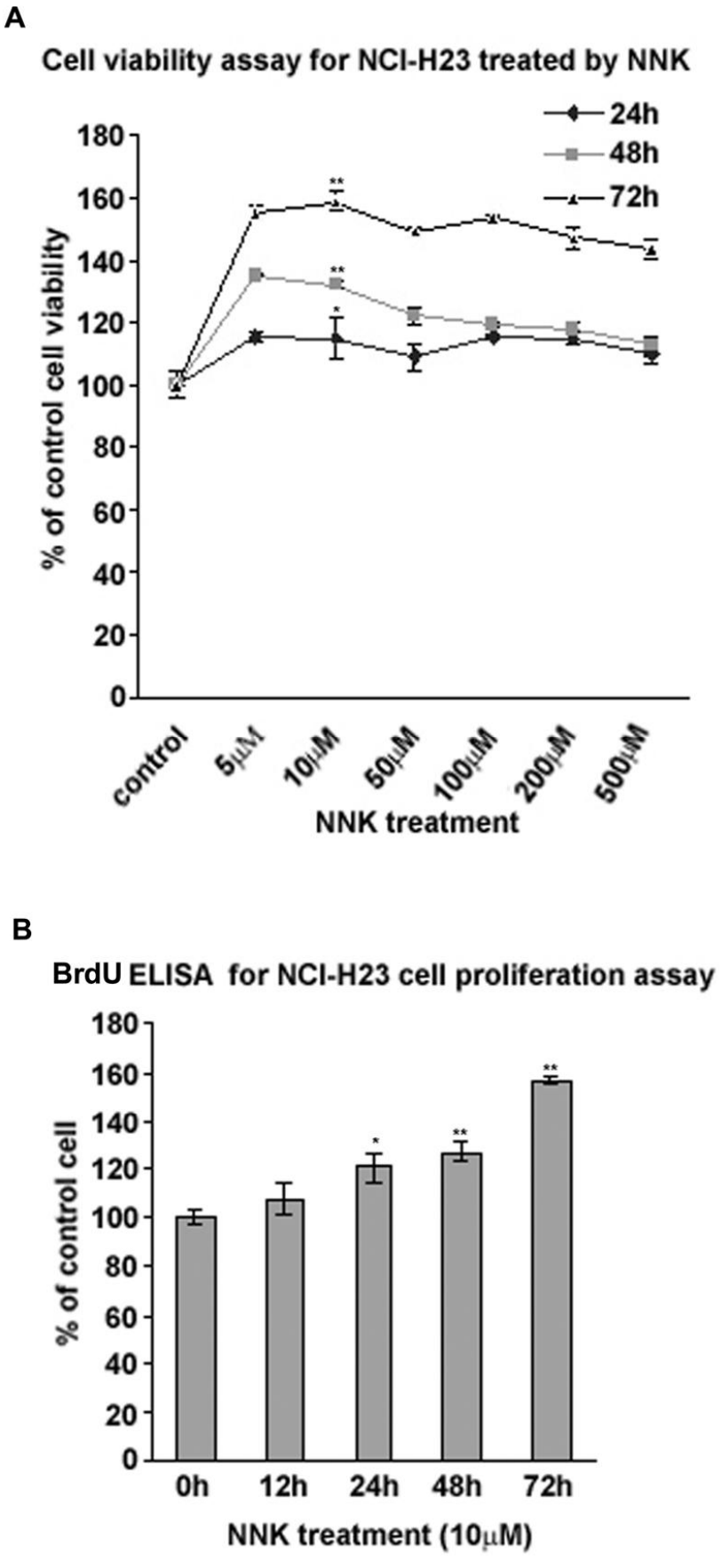
A
Cell viability assay for NCI-H23 treated by NNK
24h
48h
72h
% of control cell viability
180
160
140
120
100
80
60
40
20
0
control
5μM
10μM
50μM
100μM
200μM
500μM
NNK treatment
B
BrdU ELISA for NCI-H23 cell proliferation assay
% of control cell
180
160
140
120
100
80
60
40
20
0
0h
12h
24h
48h
72h
NNK treatment (10μM)

Fig. 3. Upregulation of the expression of HO-1, p21, CIAP-2, and Bcl-2 and downregulation of Bad in NCI-H23 cells treated by NNK. **(A)** Cells were treated with 10 μM NNK for 0 min, 1 h, 2 h, 4 h, 8 h, and 24 h. HO-1(32KD), p21 (21kD), cIAP-2(70kD), Bcl-2(28kD), and Bad(23KD) were determined by Western blot. Equal loading was confirmed by probing with antibodies against actin (43KD). The relative intensity of protein bands was summarized by column figure. The experiments were repeated twice and similar results were obtained. **(B)** Cells were treated with 10 μM NNK for 24 h. Cells without treatment were set up as control. p21 expression in the cytosol and nucleus, three kinds of phospho-Bad (Ser112, Ser136 and Ser155)(23KD) and total Bad expression were determined by Western blot. Equal loading was confirmed by probing with antibodies against actin in the cytosol and total protein and lamin B (67kD) in the nucleus. The relative intensity of protein bands was summarized by column figure. The experiments were repeated twice and similar results were obtained.

Figure 3

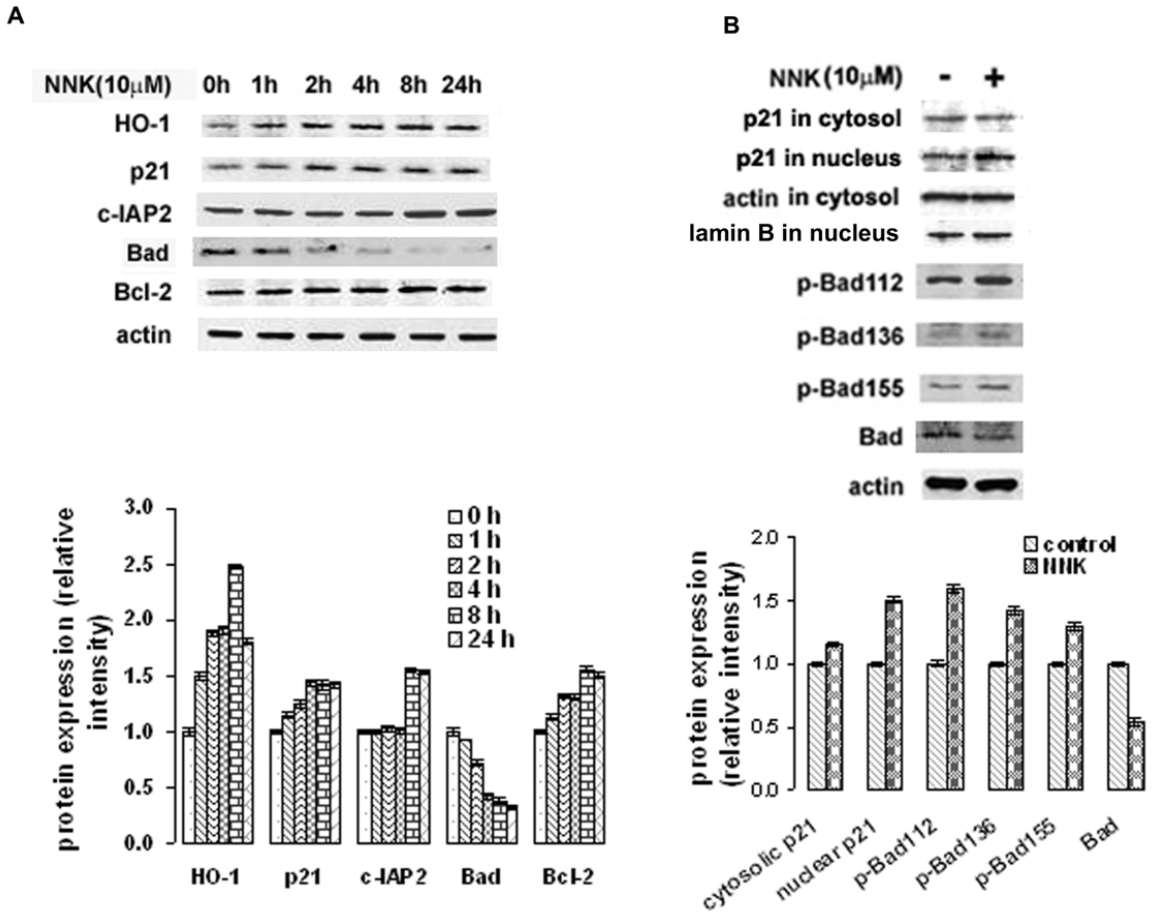

Fig. 4. Block of HO-1 prevented the effect of NNK and stimulated apoptosis. (A) Cells were treated with 10 μM NNK for 24 h, or pretreated by ZnPP XII for 30 min, followed by 10 μM NNK treatment for 24 h. Cells without treatment were set up as control. HO-1, p21, and cIAP-2 were determined by Western blot. Equal loading was confirmed by probing with antibodies against actin. The relative intensity of protein bands was summarized by column figure. The experiments were repeated twice and similar results were obtained. **(B)** The nuclear distribution of p21 in cells treated by NNK was blocked by the HO-1 inhibitor. Cells were treated by 10 μM NNK for 24 h, or pretreated by 20 μM ZnPP XII for 30 min. followed by 10 μM NNK treatment for 24 h. Two different controls were set up, untreated cells and cells treated by 20 μM ZnPP XII. An anti-p21 antibody was used in connection with an FITC

green-conjugated second antibody. DAPI (blue signal) was used for the counterstaining of the nucleus. The images were representative of the three experiments. (**C**) Block of HO-1 expression by by ZnPP XII prevented NNK-induced cell proliferation. Cells were treated with NNK 10μM, or pretreated by ZnPP XII for 30 min followed by 10 μM NNK treatment for 24 h and 48 h. Two different controls were set up, untreated cells and cells treated by 20 μM ZnPP XII. Cell proliferation was measured by MTT assay and expressed as a percentage of the control culture conditions (no treatment). The data were represented as the mean ± SD for four replicate determinations for each treatment. The experiments were repeated twice with similar results. There was a significant difference between control and NNK treated cells and between NNK treated cells and ZnPP XII plus NNK treated cells (□$p < 0.05$, ** $P < 0.01$, $n = 4$). (**D**) Block of HO-1 expression by by ZnPP XII stimulated apoptosis even in the presence of NNK. Cells were treated with NNK 10μM, or pretreated by ZnPP XII, a specific inhibitor of HO-1, for 30 min followed by 10 μM NNK treatment for 24 h. Two different controls were set up, untreated cells and cells treated by 20 μM ZnPP XII. Apoptotic result was presented as fold of 0 h control conditions (no treatment).

Figure 4A-C

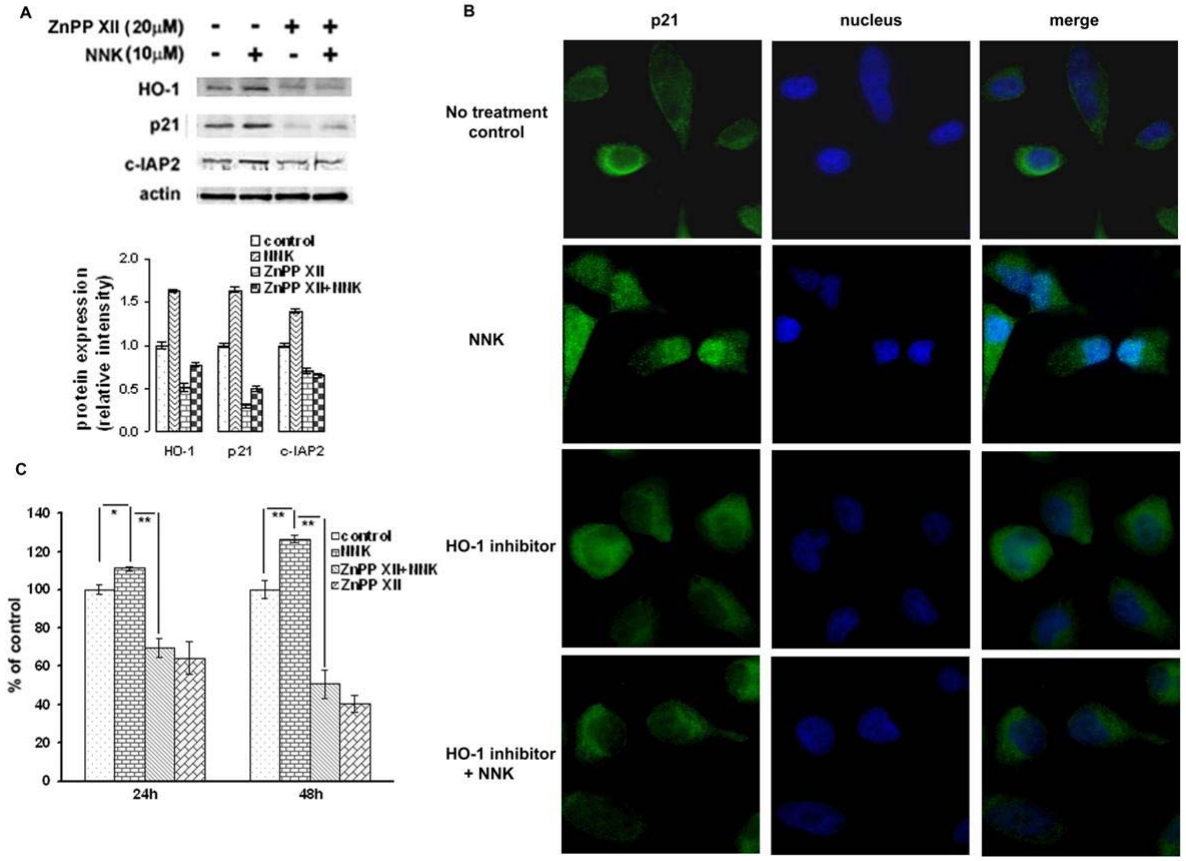
A
ZnPP XII (20μM) - - + +
NNK (10μM) - + - +
HO-1
p21
c-IAP2
actin
control
NNK
ZnPP XII
ZnPP XII+NNK
protein expression (relative intensity)
2.0
1.5
1.0
0.5
0.0
HO-1
p21
c-IAP2
B
p21
nucleus
merge
No treatment control
NNK
HO-1 inhibitor
HO-1 inhibitor + NNK
C
% of control
140
120
100
80
60
40
20
0
*
**
**
**
control
NNK
ZnPP XII+NNK
ZnPP XII
24h
48h

Figure 4D

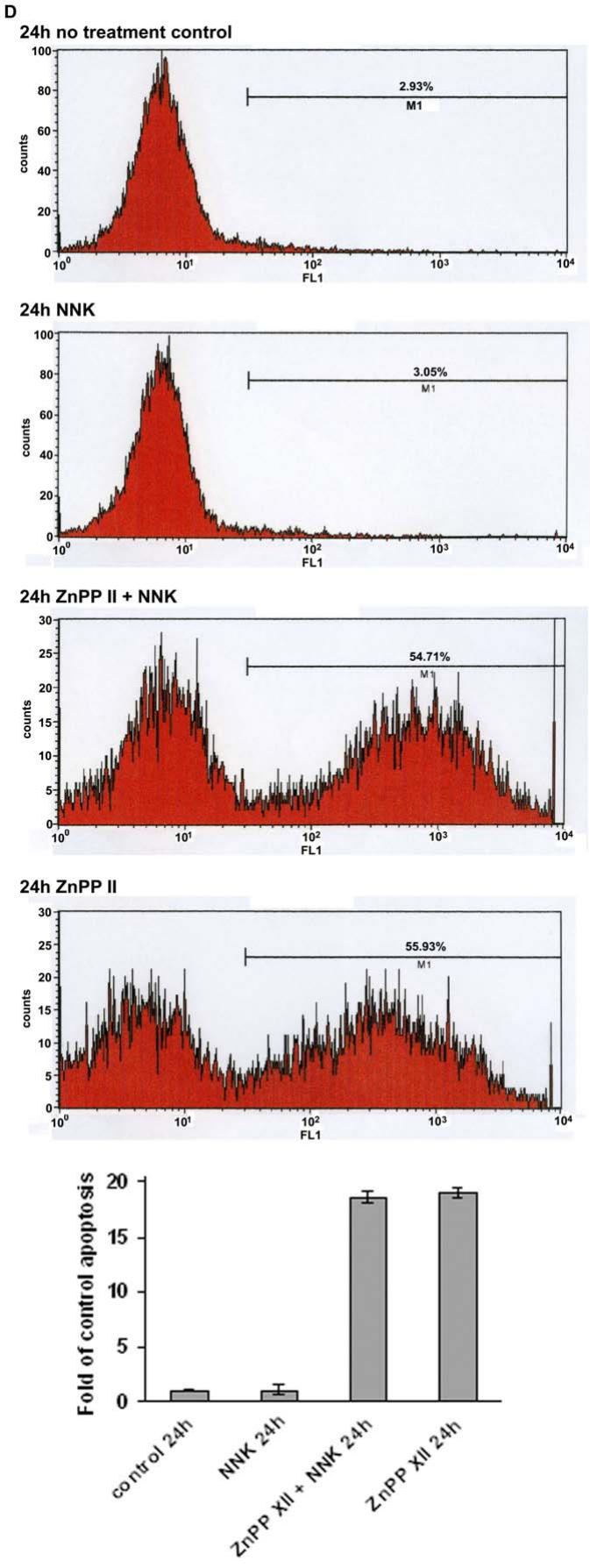
D
24h no treatment control
2.93%
M1
counts
FL1
24h NNK
3.05%
M1
counts
FL1
24h ZnPP II + NNK
54.71%
M1
counts
FL1
24h ZnPP II
55.93%
M1
counts
FL1
Fold of control apoptosis
control 24h
NNK 24h
ZnPP XII + NNK 24h
ZnPP XII 24h

Fig. 5. NNK activated NF-κB and ERK1/2. (A) Cells were treated with 10 μM NNK for 0 min, 15 min, 30 min, 60 min, 120 min, and 240 min. Western blot was done to analyze NFκB p65(65KD) in the cytosol and the nucleus, and p-IκB and IκB(37KD) in the cytosol. Equal loading was confirmed by probing with antibodies against actin in the cytosol and lamin B in the nucleus. The relative intensity of protein bands was summarized by column figure. The experiments were repeated twice and similar results were obtained. **(B)** Cells were treated with 10 μM NNK for 30 min. Cells without treatment were set up as control. An anti-p65 antibody was used in connection with a FITC green-conjugated second antibody. PI (red signal) was used for the counter-staining of the nucleus. The distribution of p65 in the cells was examined. The images are representative of the three experiments. **(C)** Cells were treated with 10 μM NNK for 0 min, 15 min, 30 min, 1 h, 2 h, 4 h, 12 h, and 24 h. The nuclear protein were extracted and applied for NF-κB transcriptional activity assay. The data were represented as the mean ± SD for four replicate determinations for each treatment. The experiments were repeated twice with similar results. **(D)** Cells were treated with 10 μM NNK for 0 min, 30 min, 60 min, and 120 min. Phospho-ERK1/2 (p-ERK1/2) protein(42/44KD), phospho-SAPK/JNK (p-SAPK/JNK) protein(46/54KD), and phospho-p38 (p-p38) protein(38KD) as well as ERK1/2(42/44KD), SAPK/JNK(46/54KD), and p38(38KD) were determined by Western blot. Equal loading was confirmed by probing with antibodies against actin. The experiments were repeated twice and similar results were obtained.

Figure 5

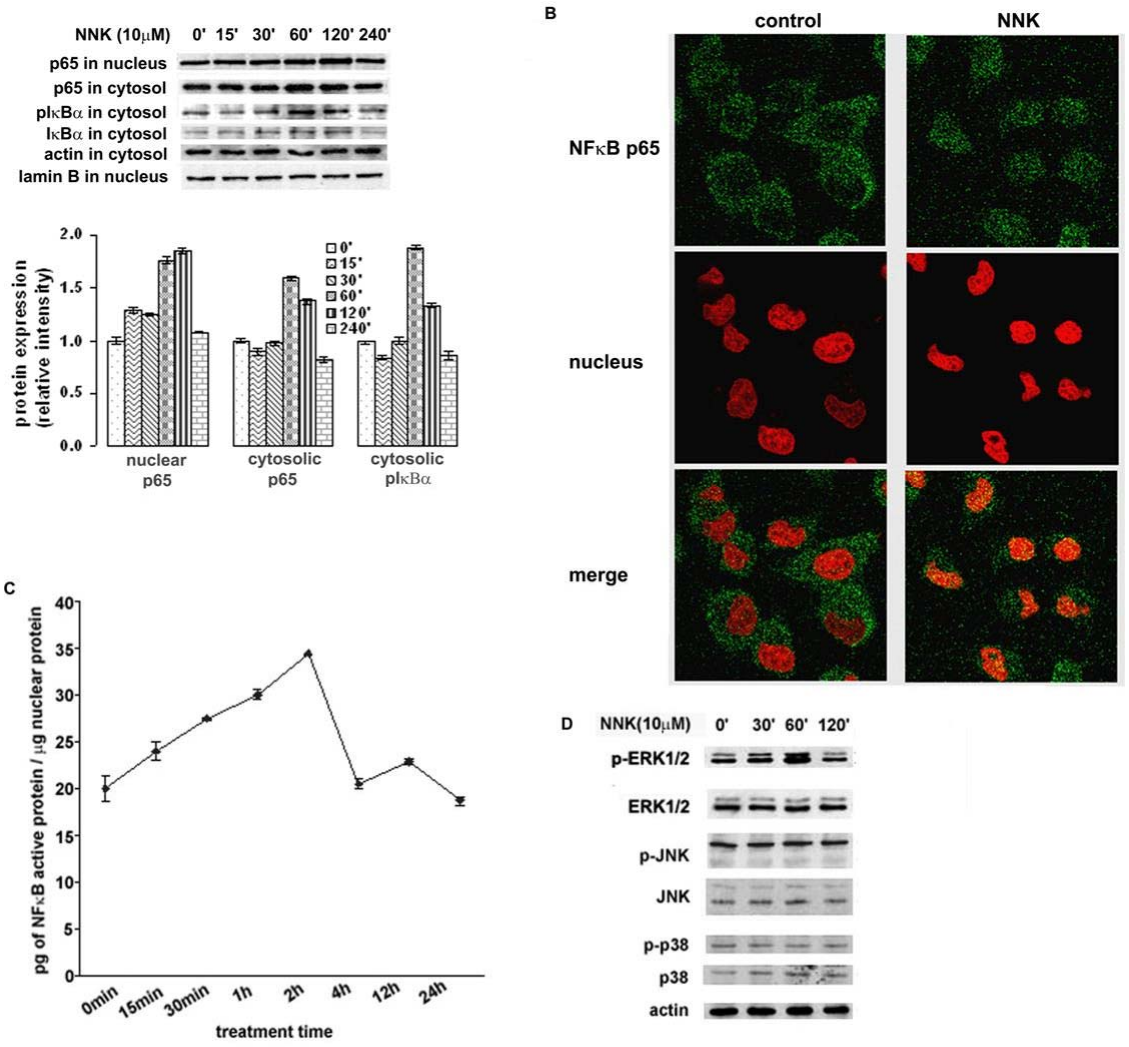

Fig. 6. Regulation of HO-1, p21, Bcl-2, Bad and cIAP-2 expression by ERK1/2 and NF-κB. (A) NCI-H23 cells were pretreated with 10 μM ERK1/2 inhibitor U0126 or 9 μM NF-κB inhibitor SN50, which was followed by 10 μM NNK treatment for 8 h and 24 h. Bcl-2 and Bad levels in the cells treated by NNK for 8 h and HO-1, p21, and cIAP-2 expression in the cells treated by NNK for 24 h were determined by Western blot. Cells without treatment were set up as control. Equal loading was confirmed by probing with antibodies against actin. The relative intensity of protein bands was summarized by column figure. The experiment was repeated twice and similar results were obtained. (**B**) Cells were pretreated

with 10 μM U0126 or 9 μM SN50 for 30 min, which was followed by 10 μM NNK treatment for 1 h. Cells without treatment were set up as control. The nuclear protein was extracted for NF-κB DNA-binding activity assay. Values (mean± SD) are expressed as the fold induction compared with the control (n=3). ** $P < 0.01$ between control and NNK-treated cells, and NNK and SN50/NNK-treated cells, respectively. *$P < 0.05$ between NNK and U0126/NNK-treated cells. **(C)** Cells were pretreated with 10 μM U0126 or 9 μM SN50 for 30 min, which was followed by 10 μM NNK treatment for 30 min. Cells without treatment were set up as control. The total protein was extracted for Western blot for p-ERK1/2 and ERK1/2. Equal loading was confirmed by probing with antibodies against actin. The experiments were repeated twice and similar results were obtained.

Figure 6